Supporting Information

Dramatic Decrease in CEST Measurement Times Using Multi-Site Excitation**

Tairan Yuwen, Lewis E. Kay, and Guillaume Bouvignies*

Author Contributions

T.Y. Conceptualization:Equal; Data curation:Equal; Formal analysis:Equal; Methodology:Equal; Software:Supporting; Visualization:Equal; Writing – original draft:Supporting
L.K. Conceptualization:Equal; Data curation:Equal; Formal analysis:Equal; Methodology:Equal; Resources:Equal; Writing – original draft:Lead
G.B. Conceptualization:Lead; Data curation:Equal; Formal analysis:Equal; Methodology:Lead; Resources:Equal; Software:Lead; Visualization:Lead; Writing – original draft:Lead

Supporting Information

Table of Contents

Intuitive Understanding of the DANTE Excitation Scheme

The evolution of starting longitudinal magnetization resulting from the application of the pulse train, $R(t)$, of Figure S1 can be understood most simply by considering the Fourier transform, FT$[R(t)]$. This, in turn, is calculated by writing the train in terms of convolutions and products of the elements indicated in this figure. Thus,

$$\begin{aligned} \mathrm{FT}[R(t)] &= \mathrm{FT}[P(t) * \{\Pi(t) \cdot \mathrm{III}(t)\}] \\ &= \mathrm{FT}[P(t)] \cdot \mathrm{FT}[\Pi(t) \cdot \mathrm{III}(t)] \\ &= \mathrm{FT}[P(t)] \cdot \{\mathrm{FT}[\Pi(t)] * \mathrm{FT}[\mathrm{III}(t)]\}. \end{aligned} \quad [S1]$$

In Eq. [S1] $P(t)$ is a rectangular pulse of duration τ_p, one of k such elements applied during the course of the DANTE scheme, $\Pi(t)$ is a rectangle with unit height and length $T = k\tau'$, the duration of the DANTE scheme, and $\mathrm{III}(t)$ is a Shah function that can be written as

$$\mathrm{III}(t) = \sum_{n=-\infty}^{\infty} \delta(t - n\tau') \quad [S2]$$

where δ is the Dirac function and τ' is the duration between the centers of the k rectangular pulses. Carrying out the Fourier transforms in Eq. [S1] we obtain,

$$\mathrm{FT}[P(t)] = \omega_1 \tau_p e^{-i\pi\Delta\nu\tau_p} \frac{\sin(\pi\Delta\nu\tau_p)}{\pi\Delta\nu\tau_p} \quad [S3]$$

where ω_1 is the strength of the B_1 field (rad/s) and $\Delta\nu$ is the offset (Hz) from the position of application of the pulse. The absorptive and dispersive mode frequency profiles can be obtained from the real ($A(\omega)$) and imaginary ($D(\omega)$) components of FT$[P(t)]$, respectively. In CEST applications the phase factor $e^{-i\pi\Delta\nu\tau_p}$ can be neglected as only the z-component of magnetization is of interest during application of the B_1 field so that in what follows we consider the magnitude, $\sqrt{A(\omega)^2 + D(\omega)^2}$,

$$\mathrm{FT}[P(t)]_{mag} = \omega_1 \tau_p \left| \frac{\sin(\pi\Delta\nu\tau_p)}{\pi\Delta\nu\tau_p} \right|. \quad [S4]$$

Note that in all of the applications considered here $\mathrm{sinc}(\pi\Delta\nu\tau_p) \sim 1$, assuming $\Delta\nu <$ 2 kHz (2 kHz is 20 ppm for ^{15}N on a 1 GHz instrument), so that Eqs. [S3, S4] reduce to

$$\mathrm{FT}[P(t)] \approx \omega_1 \tau_p. \qquad \text{[S5]}$$

It is noteworthy that when $\nu_{eff}\tau_p \ll 1$ or $\Delta\nu \gg \nu_1$, where $\nu_{eff} = \sqrt{\nu_1^2 + (\Delta\nu)^2}$, the Fourier analysis is exact, that is, it provides an identical excitation profile to that obtained from the solution of the Bloch-equations. In addition, following the above discussion,

$$\mathrm{FT}[\Pi(t)]_{mag} = T\left|\frac{\sin(\pi\Delta\nu T)}{\pi\Delta\nu T}\right|, \qquad \text{[S6]}$$

and

$$\mathrm{FT}[\mathrm{III}(t)] = \mathrm{FT}\left[\sum_{n=-\infty}^{\infty}\delta(t-n\tau')\right] = \frac{1}{\tau'}\sum_{p=-\infty}^{\infty}\delta\left(\Delta\nu - \frac{p}{\tau'}\right). \qquad \text{[S7]}$$

Note that the first null point of the $\mathrm{sinc}(x)$ function in Eq. [S6] occurs for $\Delta\nu = \pm 1/T$ and that it decays rapidly thereafter. For typical T values (> 0.3 s) this null is achieved for $|\Delta\nu| <$ 4 Hz. Thus to excellent approximation,

$$\mathrm{FT}[\Pi(t)] * \mathrm{FT}[\mathrm{III}(t)] \approx T \cdot \mathrm{FT}[\mathrm{III}(t)] \qquad \text{[S8]}$$

so that Eq. [S1] reduces to

$$\mathrm{FT}[R(t)] = \omega_1\tau_p\frac{T}{\tau'}\sum_{p=-\infty}^{\infty}\delta\left(\Delta\nu - \frac{p}{\tau'}\right). \qquad \text{[S9]}$$

Finally, recalling that $T = k\tau'$ it follows that

$$\mathrm{FT}[R(t)] = k\omega_1\tau_p\sum_{p=-\infty}^{\infty}\delta\left(\Delta\nu - \frac{p}{\tau'}\right) \qquad \text{[S10]}$$

from which it is clear that spins with resonance frequencies of p/τ', $p = 0, \pm 1, \pm 2, \ldots$ from the carrier position of the B_1 radio frequency field undergo a net rotation of $k\omega_1\tau_p$ due to the k pulses. The results from a more detailed, albeit less intuitive treatment, based on the Bloch–McConnell equations[1] are given in Figure S2.

Experimental Details

Calculating pulse lengths and the number of DANTE pulses to apply

Consider the DANTE pulse scheme of Figure S1 in which a series of k pulses of strength $B_1^{D\text{-}CEST}$ is applied over a duration T. Our goal here is to determine the values of k and τ_p so that the excited spins undergo a rotation that is equal to that in a 'typical' CEST experiment in which a continuous radio frequency field of strength B_1^{CEST} is applied for the total duration T. As described in the previous section the effect of the DANTE scheme is to excite spins that are separated in frequency by p/τ', $p = 0, \pm1, \pm2, \ldots$; these spins can effectively be treated as 'on-resonance', so that the net flip angle, θ (rad), is simply given by $\theta = 2\pi k B_1^{D\text{-}CEST}\tau_p$ (Eq. [S10]). Thus,

$$\begin{aligned} 2\pi k B_1^{D\text{-}CEST}\tau_p &= 2\pi B_1^{CEST} T \\ k\tau' &= T \end{aligned} \qquad [S11]$$

from which it follows directly that

$$\tau_p = \frac{B_1^{CEST}}{B_1^{D\text{-}CEST}}\tau' \qquad [S12]$$

where $1/\tau'$ is the spacing in frequency space (Hz) between points of excitation (referred to in what follows and in the main text as the spectral width, sw_{CEST}). Both k and τ_p are set by the pulse program (included below) automatically based on the length of the CEST element and the strength of applied pulses relative to the effective B_1 field in the equivalent CEST experiment where continuous low power irradiation is used (Eq. [S11]).

Calculating the ^1H decoupling field strength during T

During the CEST element it is often desirable to remove scalar-coupling interactions that would otherwise split the CEST dips, thereby decreasing sensitivity. In the case of ^{15}N-CEST, decoupling of the one-bond ^{1}H–^{15}N scalar coupling is easily accomplished by using the ^{1}H $90_x240_y90_x$ composite decoupling sequence,[2] as described

previously.[3] Very small 'decoupling artifact' dips are generated, displaced by frequencies of $\pm\frac{jB_1^H}{2.33}$ Hz from the main dip where j is a whole number and B_1^H is the ^{1}H field strength (Hz). In applications of CEST considered to this point the positions of the decoupling artifacts have typically fallen outside of the ^{15}N chemical shift window and so are not problematic.[3] In contrast, in the D-CEST scheme introduced here the effective spectral window in the CEST dimension, $sw_{CEST} = 1/\tau'$, is significantly reduced, so that aliasing of artifactual dips does occur, in a similar manner to aliasing of the exchange dips of interest. In order to avoid complications that might occur we prefer to adjust B_1^H slightly so that all decoupling dips are aliased on top of the major dip. This can be achieved by setting B_1^H such that

$$\frac{B_1^H}{2.33} = l \cdot sw_{CEST} \qquad \text{[S13]}$$

where l is a whole number chosen such that the strength of B_1^H is changed as little as possible from the desired value. Typically B_1^H values on the order of 3.5 kHz are employed so that for a sw_{CEST} value of 700 Hz a small adjustment of B_1^H to 3.26 kHz would be required, corresponding to $l = 2$ in Eq. [S13]. A value for l is automatically set by the pulse program once an approximate B_1^H value is chosen and the actual B_1^H determined from that.

Choice of appropriate sw_{CEST} values

As described in the main text, a pair of D-CEST experiments is recorded with different sw_{CEST} values (different pulse spacing in the time domain, Figure 1a) so that degeneracies in the chemical shifts of excited state spins can be resolved. It is of interest to ask if special care must be taken in the choice of the D-CEST spectral widths or if there are occasions when ambiguities in chemical shifts still remain, even with a pair of experiments. Consider the case where D-CEST datasets are recorded with distinct spectral widths of sw_a and sw_b, $sw_a > sw_b$, such that the position of $B_1^{D\text{-}CEST}$ is varied between $(-sw_a/2, +sw_a/2)$ or $(-sw_b/2, +sw_b/2)$ in a series of spectra. Further, we define sw_j such that sw_j is the lowest common multiple of (sw_a, sw_b), for example,

$sw_j = 3000$ Hz for $(sw_a, sw_b) = (600, 500)$ Hz. In what follows we focus on a spin that resonates at a frequency ζ removed from the center of the spectral window. In the case where $\zeta \in (-sw_b/2, +sw_b/2)$ the peak is not aliased in either dataset and would, of course, be at the same position in both spectra. In the general case we might find, however, a peak at positions α and β when $sw_{CEST} = sw_a$ and sw_b, respectively, where $\alpha \in (-sw_a/2, +sw_a/2)$ and $\beta \in (-sw_b/2, +sw_b/2)$. Note that if only a single dataset is recorded there would be an infinite number of possible values for ζ corresponding to $\alpha + x \cdot sw_a$ or $\beta + y \cdot sw_b$, depending on whether $sw_{CEST} = sw_a$ or sw_b, with x and y integers. By recording both datasets we restrict the number of solutions to those simultaneously satisfying the relations

$$\begin{cases} \zeta - x \cdot sw_a = \alpha \\ \zeta - y \cdot sw_b = \beta \end{cases}. \qquad \text{[S14]}$$

However, even with two datasets there still remains an infinite number of solutions since potential resonance frequencies $\zeta \pm p \cdot sw_j$ cannot be distinguished from each other (p is a whole number), with each resulting in a peak aliased at exactly the same location in the spectral window that is observed. That is if (x_i, y_i) is a solution to Eq. [S14] then so too is $\left(x_i \pm \frac{p \cdot sw_j}{sw_a}, y_i \pm \frac{p \cdot sw_j}{sw_b} \right)$. However, sw_a and sw_b can be chosen judiciously such that sw_j is sufficiently large so that only $p = 0$ is physically reasonable (*i.e.*, $p \cdot sw_j$ lies outside the frequency range for the spin-type in question).

The judicious choice of a pair of sw_{CEST} values, as described above, does not insure that minor and major state dips never superimpose, however. Aliasing of one dip on top of the other will occur when the shift difference between spins in the major and minor conformations is an integer multiple of sw_{CEST}. In this case the choice of a pair of sw_{CEST} values is critical, since although overlap may occur for sw_a, for example, it will then not occur for sw_b. The combined analysis of both datasets allows for the unambiguous determination of the position of the minor dips, as in general. This situation is illustrated for L42 in Figure S6 where major and minor dips overlap for sw_{CEST} = 700 Hz but not 800 Hz.

Choice of B_1 frequency offsets

D-CEST datasets should generally be collected using a set of B_1 offset frequencies covering a range equal to sw_{CEST} with an interval between consecutive offsets approximately equal to the average B_1 field strength expressed in Hz ($B_1^{D\text{-}CEST}\frac{\tau_p}{\tau'}$); such spacing ensures that dips are sampled with sufficient resolution.[4] For example, for an average B_1 field of 20 Hz and sw_{CEST} = 600 Hz, an appropriate sampling scheme would be $\{-300, -280, \ldots, -20, 0, 20, \ldots, 280, 300\}$ Hz. Note that, in this case, the first and last offsets are exactly separated by sw_{CEST} and, therefore, can be considered as duplicate points due to the inherent sw_{CEST}-periodicity of the D-CEST profile. Thus, it is not essential to measure both of them. However, we believe that it is a good practice to do so if only for checking whether the experiment is set up correctly.

As described in the previous section, multiple D-CEST datasets with differing sw_{CEST} values must be collected in order to 'uniquely' define the chemical shift of the resonances of interest. As most CEST studies usually involve the measurement of multiple datasets with different B_1 field strengths, a convenient way of recording data is to collect each D-CEST dataset, associated with a specific B_1 field strength, with a different sw_{CEST} value. However, in the specific case where data from only one B_1 field is required, a second experiment where sw_{CEST} is the only varied parameter could potentially be highly redundant with many of the same frequency positions irradiated in both experiments. For example, such a situation would arise in the case where $sw_{CEST} = sw_a, sw_b$ are chosen where the frequency spacing is given by $(\frac{sw_a - sw_b}{2p})$ spanning $[-sw_a/2, +sw_a/2]$ and $[-sw_b/2, +sw_b/2]$ and p is a whole number. One way to avoid this potential redundancy is, in fact, to choose the frequency spacing as defined above $(\frac{sw_a - sw_b}{2p})$, but to collect odd and even offset frequencies in two separate experiments, each obtained with a different sw_{CEST}. Note that a single D-CEST experiment recorded using sw_{CEST} = 600 Hz and offset frequencies of $\{-300, -280, \ldots, -20, 0, 20, \ldots, 280, 300\}$ Hz irradiates the same positions as the combination of two experiments recorded using sw_{CEST} = 600 Hz and 560 Hz and the offset frequencies $\{-300, -260, \ldots, -20, 20, \ldots, 260, 300\}$ Hz and

$\{-280, -240, \ldots, -40, 0, 40, \ldots, 240, 280\}$ Hz, respectively. Thus, all of the 20 Hz spaced B_1 fields are contained within the pair of datasets and there is no increase in experimental time over recording only a single experiment containing all 20 Hz separated frequencies.

Relative average power dissipated by CEST and D-CEST

Average powers over the length of the CEST element can be calculated from

$$\begin{aligned} P_{avg}^{CEST} \cdot T &= \lambda (B_1^{CEST})^2 T \\ P_{avg}^{D\text{-}CEST} \cdot T &= \lambda (B_1^{D\text{-}CEST})^2 \tau_p k \end{aligned} \qquad [S15]$$

where λ is a constant. Thus,

$$\frac{P_{avg}^{D\text{-}CEST}}{P_{avg}^{CEST}} = \frac{(B_1^{D\text{-}CEST})^2 \tau_p k}{(B_1^{CEST})^2 T} = \left(\frac{B_1^{D\text{-}CEST}}{B_1^{CEST}}\right)^2 \frac{\tau_p}{\tau'} = \frac{B_1^{D\text{-}CEST}}{B_1^{CEST}}. \qquad [S16]$$

For typical B_1 values ($B_1^{D\text{-}CEST}$ = 6000 Hz, B_1^{CEST} = 20 Hz) $\frac{B_1^{D\text{-}CEST}}{B_1^{CEST}} \sim 300$, so that the D-CEST experiment deposits ~300 fold more average power into the sample than the standard CEST scheme. For reference on one of our cryo-probes a B_1^{CEST} field of 25 Hz corresponds to 0.0015 W so that an average power of ~0.5 W is deposited using the DANTE scheme with pulses applied at the highest possible power.

NMR samples

Both G48A Fyn SH3 and A39G FF domains were expressed and purified as described in previous studies.[3,5] The G48A Fyn SH3 domain sample was 1.5 mM [U-^{15}N]-labeled protein dissolved in 50 mM sodium phosphate (pH 7.0), 0.2 mM EDTA, 0.02% NaN_3 and 90% H_2O/10% D_2O. The NMR sample of A39G FF domain was prepared at a concentration of 2 mM [U-^{15}N]-labeled protein in 50 mM sodium acetate (pH 5.7), 100 mM NaCl and 90% H_2O/10% D_2O.

NMR spectroscopy

All experiments measured on G48A Fyn SH3 were performed at 25 °C using a 1 GHz Avance III Bruker spectrometer equipped with a cryogenically cooled probe with a z-axis gradient. A regular ^{15}N-CEST dataset was recorded using the standard pulse scheme, described previously,[3] with a weak B_1 field of ~20 Hz and a relaxation delay, T, of 200 ms. A total of 133 2D planes were collected in an interleaved manner, corresponding to B_1 field positions that varied from 104 ppm to 137 ppm (*i.e.*, from −1500 to 1800 Hz about 118.7 ppm) with a step-size of 25 Hz. A pair of ^{15}N D-CEST experiments was measured with the pulse sequence of Figure S4 using sw_{CEST} values of 700 Hz and 800 Hz, an effective B_1 field of ~20 Hz and T = 200 ms. For sw_{CEST} = 700 Hz (800 Hz) the pseudo-3D datasets contained 15 (17) 2D planes, respectively, with the carrier position of the DANTE pulse scheme placed every 50 Hz, in the range from −375 to 325 Hz (from −400 to 400 Hz) centered about 118.7 ppm. Note that the sets of sampled positions in the D-CEST experiments were chosen to be non-overlapping (see text and discussion above "*Choice of B_1 frequency offsets*"), with the same set of frequencies irradiated in total as in the standard CEST experiment. Each dataset was measured with 2 transients per FID, 80 complex t_1 points, acquisition times of (55, 70) ms in (t_1, t_2) along with a pre-scan delay of 1.7 s, for a net acquisition time of ~11 min per plane and total acquisition times of ~24.5 h (CEST), ~2.9 h (D-CEST, sw_{CEST} = 700 Hz) and ~3.3 h (D-CEST, sw_{CEST} = 800 Hz).

CEST and D-CEST experiments recorded on the A39G FF sample were obtained at 1 °C using an 800 MHz Avance III Bruker spectrometer equipped with a cryogenically cooled probe with a z-axis gradient. A regular ^{15}N CEST dataset comprising 102 2D planes was measured with a weak ^{15}N B_1 field of 20.25 Hz by varying the ^{15}N CEST field position in the range 107–131 ppm with a step-size of 20 Hz. ^{15}N D-CEST datasets were recorded using an average B_1 field of 4.95 Hz and the ^{15}N D-CEST field position was varied over 240 Hz with a step-size of 5 Hz to generate a pseudo-3D CEST dataset containing 50 2D planes in total. In both experiments, a CEST period of $T = 1000$ ms was used, each 2D plane was recorded with two transients per FID, the pre-scan delay

was 2.5 s and 64 complex points in t_1 were recorded, to give a net acquisition time of ~16 min per spectrum. Measurement times for regular CEST and D-CEST experiments were ~26 h and ~13 h, respectively.

Each dataset was recorded along with a reference plane, where the CEST or D-CEST relaxation period, T, was omitted, so as to obtain robust estimates of longitudinal relaxation rates. Calibration of the weak (average) ^{15}N B_1 field strengths in CEST (D-CEST) experiments followed the approach of Guenneugues *et al.*[6]

Data analysis

All spectra were processed and analyzed using the NMRPipe software suite[7] and visualized with the program SPARKY.[8,9] Analyses of CEST and D-CEST profiles were carried out using the software package ChemEx (https://github.com/gbouvignies/chemex) that simulates the experiment by propagating a Bloch–McConnell Liouvillian[1,10] and minimizes a standard χ^2 cost function to obtain the best-fit parameters, as described in detail previously.[3] For the analysis of D-CEST datasets, a separate ChemEx module that calculates the magnetization trajectory over the DANTE pulse scheme was implemented and used; it is now part of ChemEx. All datasets were analyzed globally (all sites together) using a two-site exchange model, $G \rightleftharpoons E$, to obtain the fractional population of the minor state, p_E, and the exchange rate between the ground (G) and the excited (E) states, $k_{ex} = k_{GE} + k_{EG}$. Site-specific fitting parameters were $\{\varpi_G, \varpi_E, R_{2,G}, R_{2,E}, R_1\}$, where ϖ_i is the chemical shift of a nucleus in state i (ppm), $R_{2,i}$ is its transverse relaxation rate (s^{-1}) and R_1 is its longitudinal relaxation rate (s^{-1}), the latter assumed to be common to both states. Note that the D-CEST profiles recorded on G48A Fyn SH3, measured with a pair of sw_{CEST} values (700 and 800 Hz), were jointly fit. B_1 field inhomogeneity effects were taken into account in the fit by generating an averaged profile in which individual profiles for each of 10 B_1 field values evenly spaced within $\pm 2\sigma$ about the mean, where σ is the standard deviation of the B_1 field distribution, were calculated. These were subsequently weighted and averaged assuming a Gaussian distribution and used to fit the experimental data. A B_1 field inhomogeneity

of 10% was assumed in all calculations.

Simulation of D-CEST profiles requires the calculation of a pair of propagators, including one for the DANTE pulse of duration τ_p and a second that evolves magnetization during a subsequent delay τ during which *rf* is not applied. This is twice more than what is required for calculating CEST datasets, potentially making the calculation two-fold slower. However, the increase in calculation time is often counterbalanced by the fact that D-CEST datasets usually contain many less points than their CEST counterparts. It is worth noting that in both cases the computations are much more rapid than for the corresponding CEST profiles that exploit cosine-modulated schemes, where calculations must be performed on a point-by-point basis during excitation.[11]

Initial guess of the minor state positions

In order to avoid traps in local minima during the fitting procedure good initial guesses for the minor state resonance frequencies, ϖ_E, are required. For regular CEST data these are readily available from a rapid inspection of the CEST profiles. However, as described in the text and above, there are ambiguities in the positions of the minor state dips recorded via the D-CEST approach because of the potential of aliasing. An initial guess for ϖ_E can be readily achieved by superimposing two or more profiles recorded using different sw_{CEST} values and extrapolating them over the complete chemical region of interest assuming perfect periodicity (see Figure S3). The position where the minor dips of all profiles superimpose must necessarily correspond to the frequency of the minor state resonance, as illustrated by the comparison of the CEST and (extrapolated) D-CEST profiles in Figure S3. The approach was implemented in a Python based program and includes a graphical interface, where the extrapolated D-CEST profiles are plotted and the user is invited to click on the positions corresponding to the exchanging resonances. In addition to this visual (manual) mode, the program also offers an option to automatically localize the major and minor resonances. The software is available upon request.

Supporting Figures

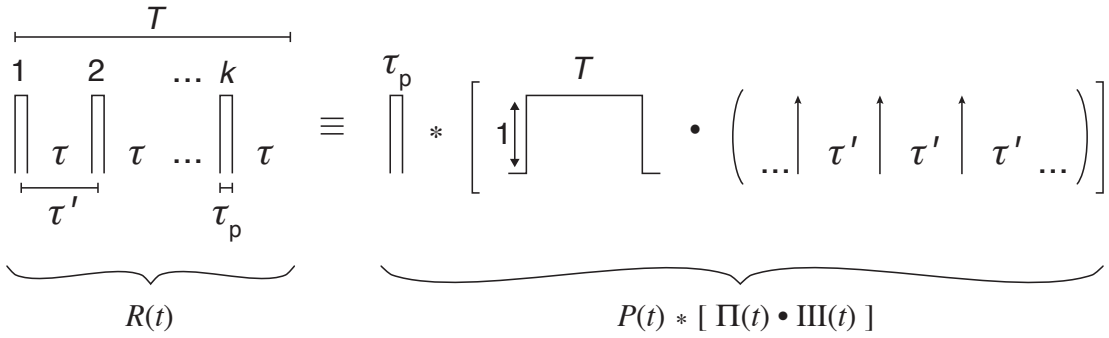

Figure S1. The DANTE pulse scheme, $R(t)$, can be expressed in terms of the convolution of a rectangular pulse of duration τ_p ($P(t)$), with an element that, in turn, is given by the product of a rectangular pulse of unit height and length T ($\Pi(t)$) and a set of Dirac pulses separated by delay τ' ($\mathrm{III}(t)$).

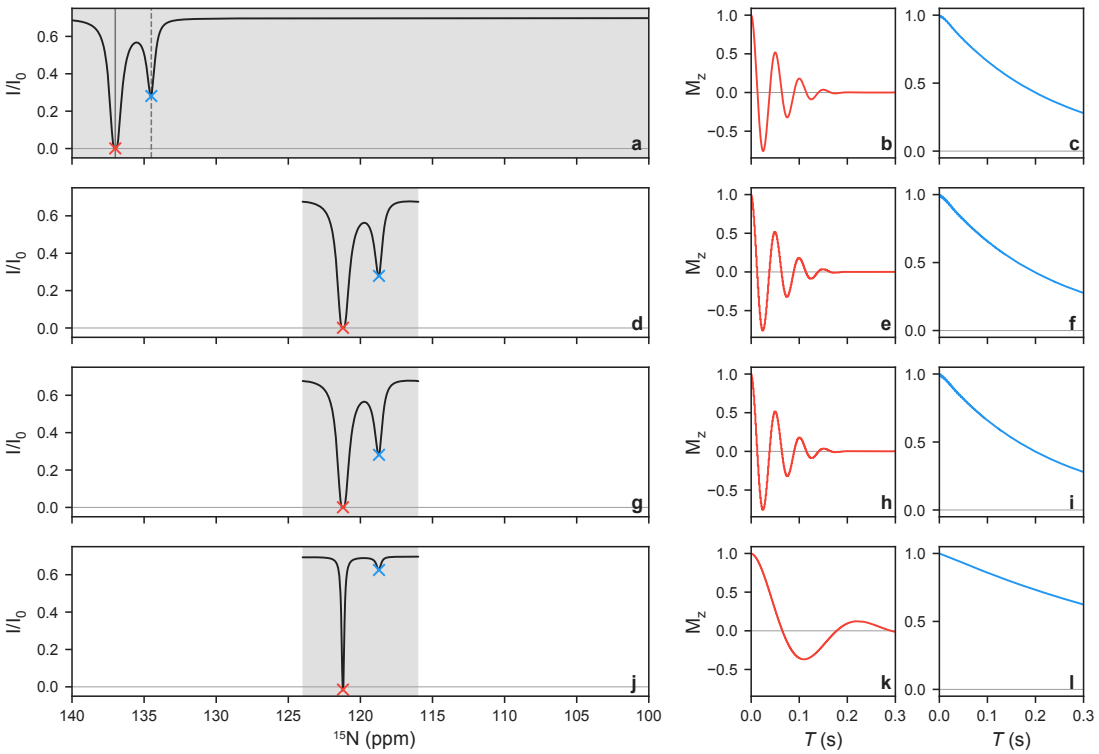

Figure S2. Comparison of the performance of D-CEST relative to CEST (**a**, **b**, **c**) for $B_1^{D\text{-}CEST}$ = 5 kHz (**d**, **e**, **f**), 500 Hz (**g**, **h**, **i**) and 50 Hz (**j**, **k**, **l**). All simulations were based on a two-site exchange model using the Bloch–McConnell equations[1] with $p_E = 5\%$, k_{ex} = 100 s^{-1}, R_1 = 1.2 s^{-1}, R_2 = 10 s^{-1}, a CEST exchange period of total duration T = 300 ms and a static magnetic field of 23.5 T. B_1 inhomogeneity was taken into account as described above, assuming a value of 10% in all simulations. The solid and dashed gray lines denote the resonance positions of the spin of interest in the ground and excited states, respectively. To generate the profiles in (**a**, **d**, **g**, **j**) the frequency range shown in gray was swept. Note that in the D-CEST profiles (**d**, **g**, **j**) the major and minor dips are aliased from 137 ppm and 134.5 ppm, respectively, and excitation occurs via a DANTE sideband that is $2sw_{CEST}$ displaced from the carrier frequency. For applications where the $B_1^{D\text{-}CEST}$ field is 5 kHz or 500 Hz there is no distortion of the resultant profile but for weak fields such as 50 Hz a significant distortion occurs that reflects the weak DANTE pulses used. Panels on the right correspond to the trajectory of z-magnetization at positions indicated by × in the profiles (left). It is clear, both from profiles and magnetization trajectories, that CEST and D-CEST are equivalent when $B_1^{D\text{-}CEST}$ = 5 kHz or 500 Hz, while significant artifacts are introduced for weak $B_1^{D\text{-}CEST}$ values such as 50 Hz. In all simulations the effective B_1 was 20 Hz, so that the net nutation of magnetization over the total CEST/D-CEST element was the same.

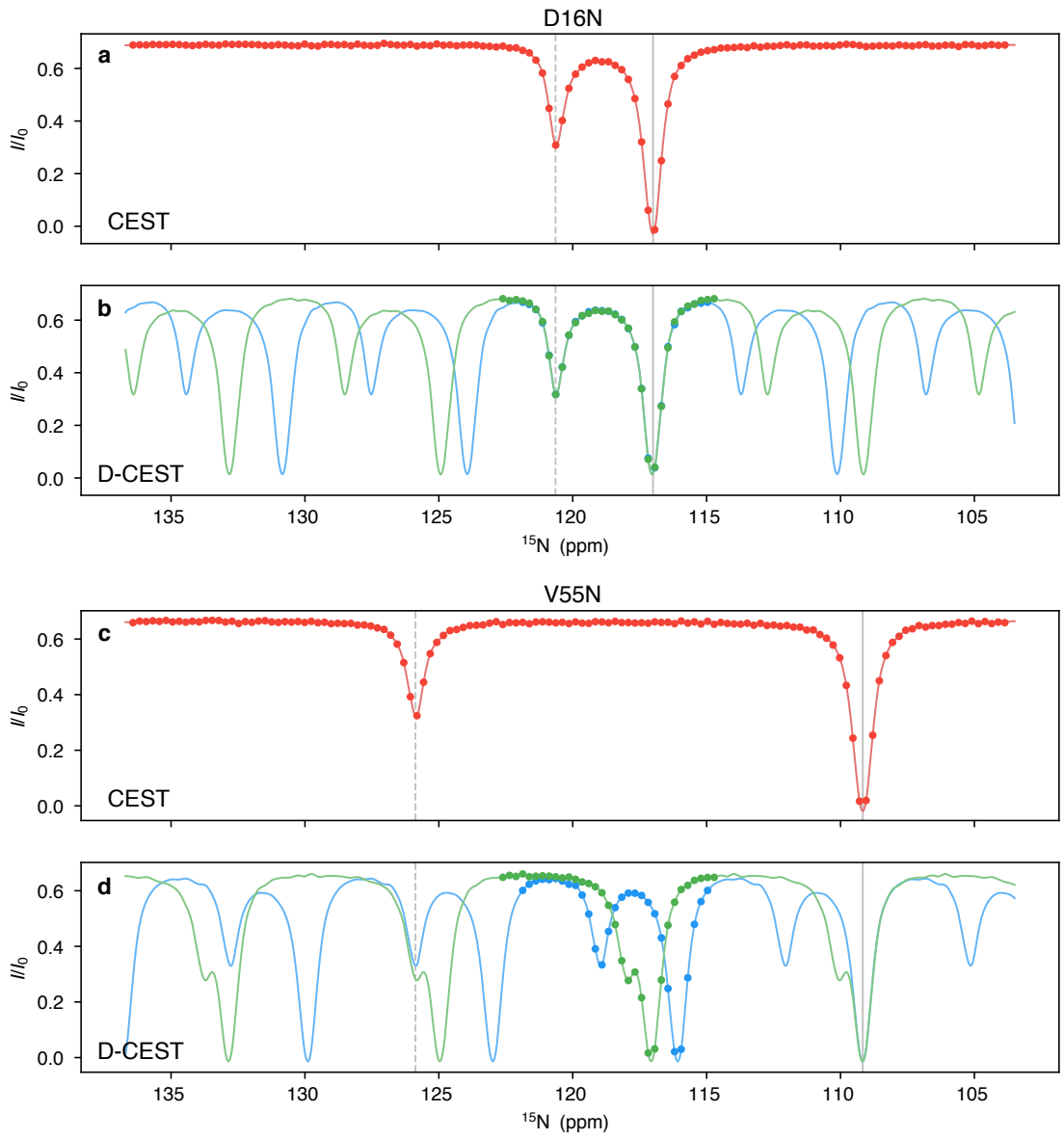

Figure S3. The minor state resonance position can be visually inferred from a comparison of D-CEST profiles recorded with different values of sw_{CEST}. Experimental ^{15}N-CEST profiles of residues D16 (**a**, **b**) and V55 (**c**, **d**) of G48A Fyn SH3 acquired at 25 °C, 23.5 T, using the standard ^{15}N-CEST pulse sequence (red) (**a**, **c**) and the ^{15}N D-CEST pulse sequence with sw_{CEST} set to 700 Hz (blue) and 800 Hz (green) and centered at 118.7 ppm (**b**, **d**). All experiments were recorded using an effective B_1 field of 20 Hz. Experimental data points are shown with circles and solid lines represent a cubic spline interpolation of the data, extrapolated over the complete ^{15}N range relevant for backbone amides in proteins assuming a periodicity of sw_{CEST} for the D-CEST profiles. The positions of the major and minor state resonances are highlighted by solid and dashed vertical gray lines, respectively, and are at positions corresponding to the overlap of dips (blue and green) in profiles recorded at the pair of sw_{CEST} values.

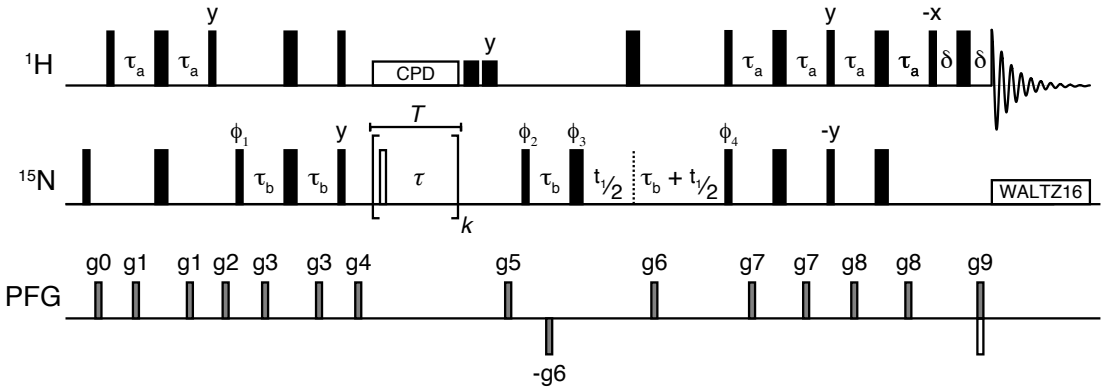

Figure S4. D-CEST based pulse scheme for recording ^{15}N-CEST profiles. The sequence is identical to a previously published version for recording ^{15}N-CEST data,[3] except that a ^{15}N DANTE excitation scheme is used in place of the weak ^{15}N continuous-wave (CW) field that is applied in regular CEST experiments. The DANTE scheme is composed of k rectangular pulses of duration τ_p (white rectangle), each followed by a delay (τ) for a total duration $T = k(\tau_p + \tau)$, see Figure S1. Further details regarding the pulse sequence can be found in a previous study[3] or in the attached pulse sequence code.

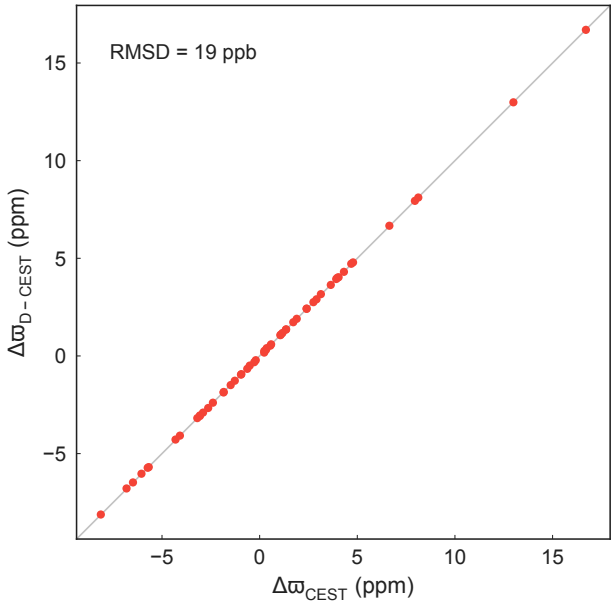

Figure S5. Linear correlation plot of ^{15}N chemical shift differences (ppm) between nuclei in the ground and the excited states of G48A Fyn SH3 obtained from analysis of ^{15}N CEST ($\Delta\varpi_{CEST}$) and ^{15}N D-CEST ($\Delta\varpi_{D\text{-}CEST}$) experiments, 25 °C.

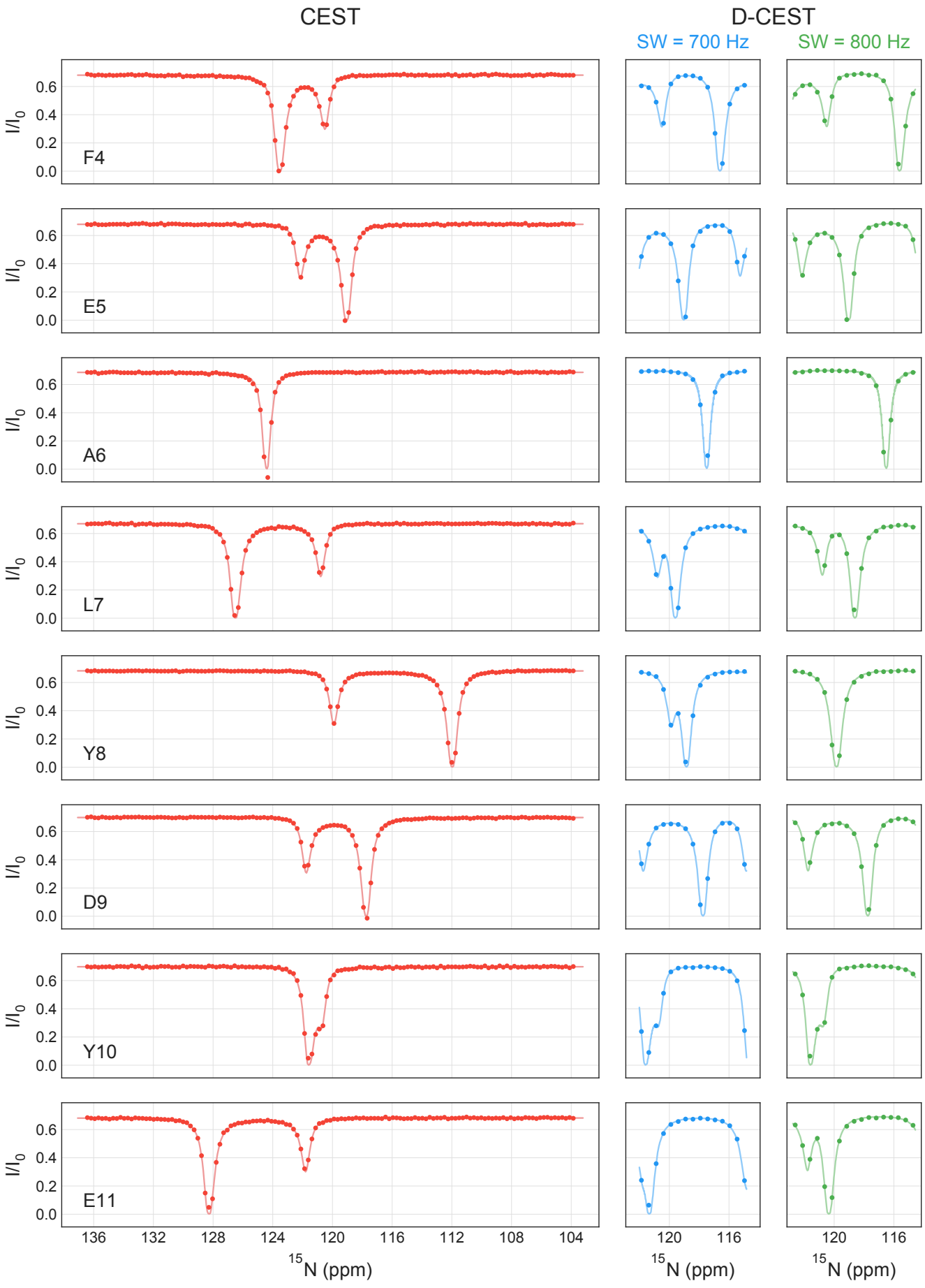
CEST
D-CEST
SW = 700 Hz
SW = 800 Hz
I/I0
F4
E5
A6
L7
Y8
D9
Y10
E11
0.0
0.2
0.4
0.6
136
132
128
124
120
116
112
108
104
15N (ppm)

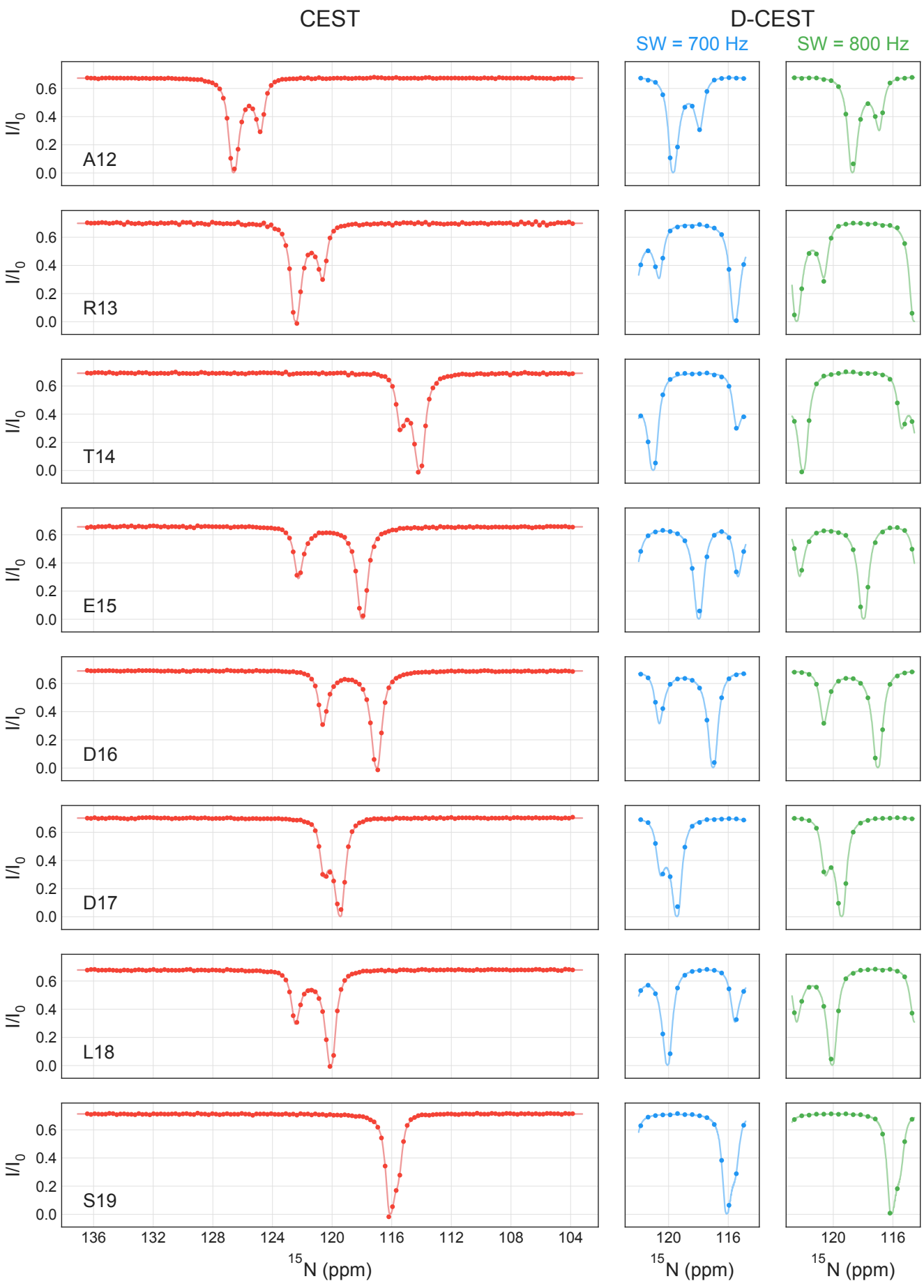
CEST
D-CEST
SW = 700 Hz
SW = 800 Hz
I/I0
A12
R13
T14
E15
D16
D17
L18
S19
0.0
0.2
0.4
0.6
136
132
128
124
120
116
112
108
104
15N (ppm)

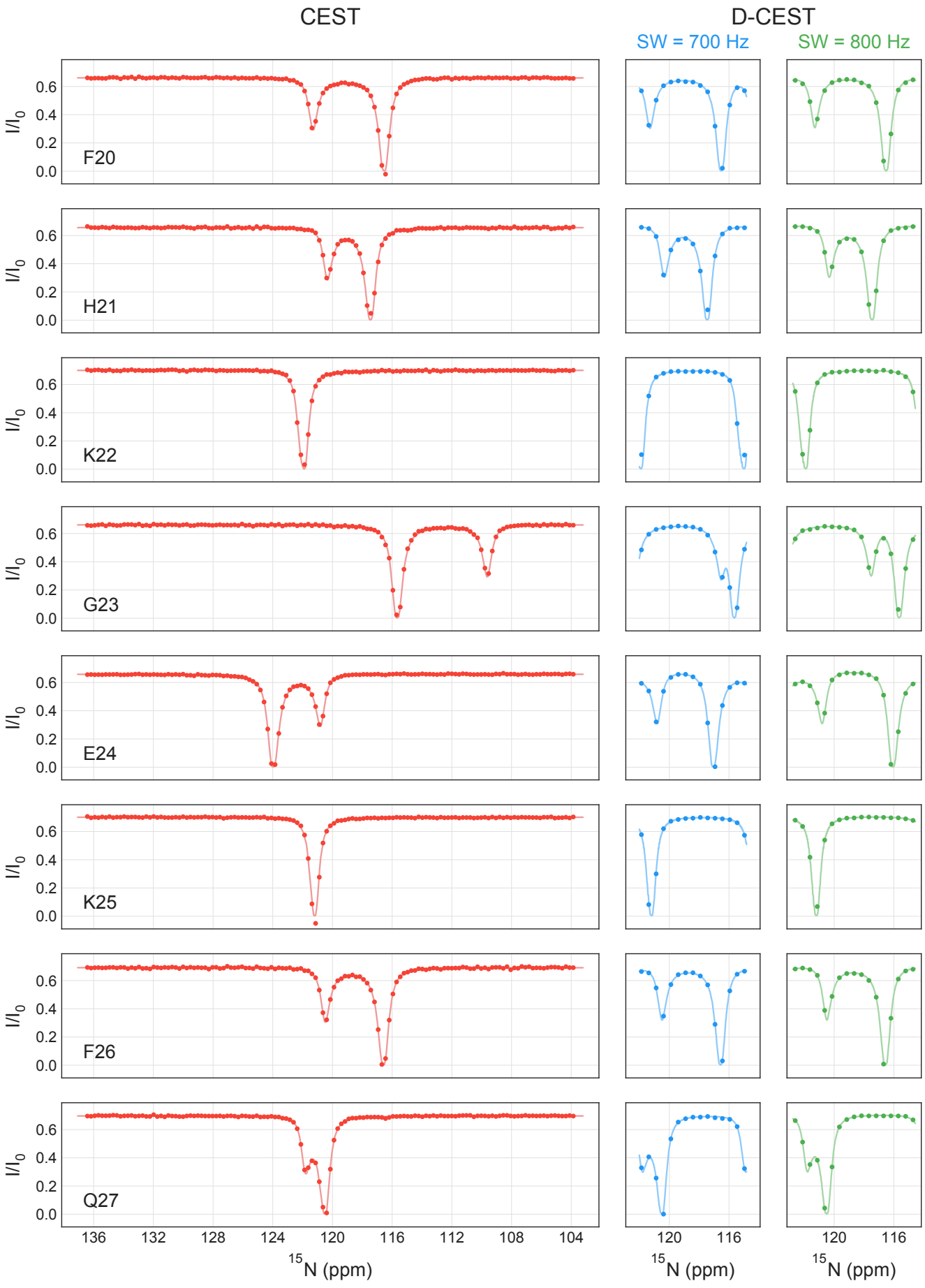
CEST
D-CEST
SW = 700 Hz
SW = 800 Hz
I/I0
F20
H21
K22
G23
E24
K25
F26
Q27
0.0
0.2
0.4
0.6
136
132
128
124
120
116
112
108
104
15N (ppm)

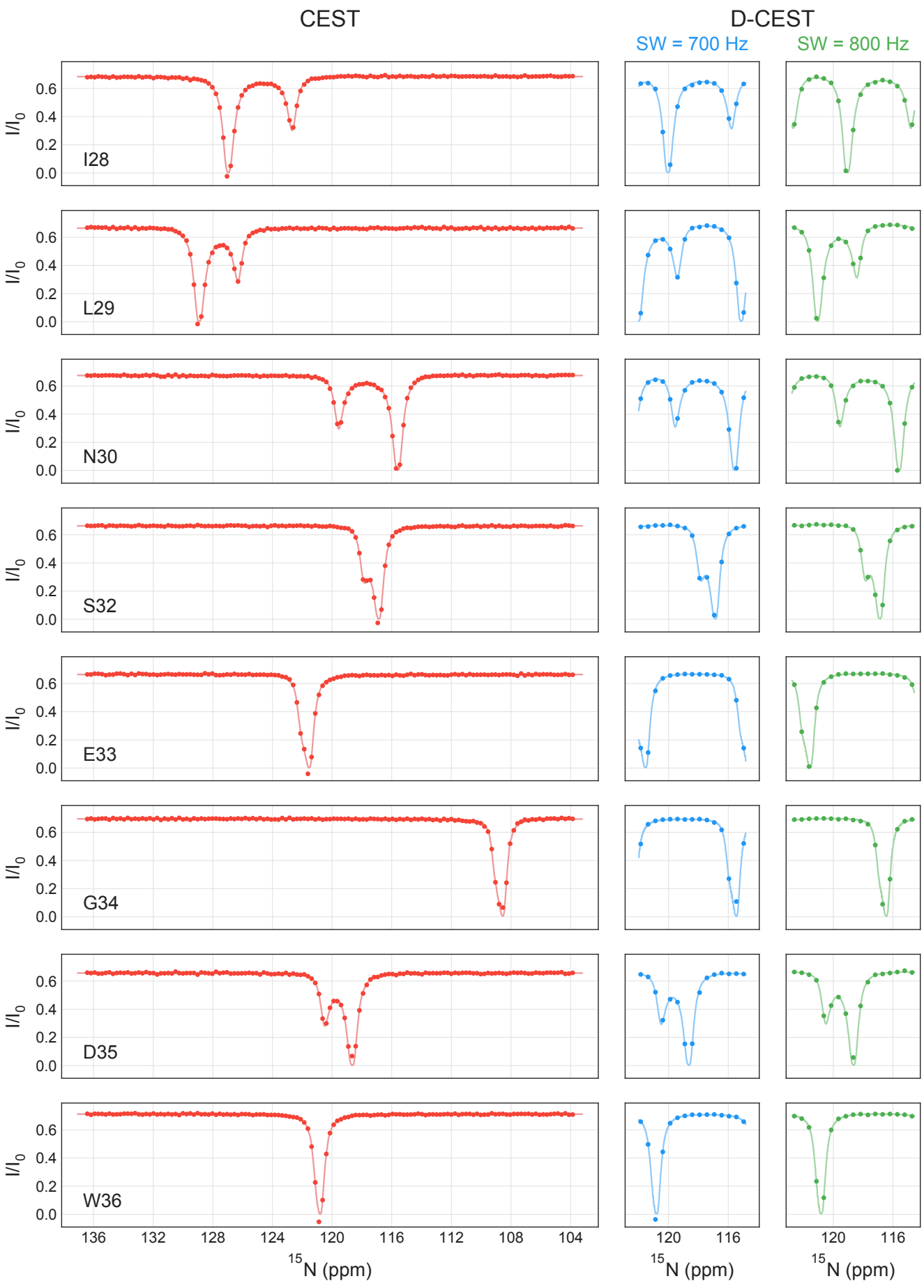
CEST
D-CEST
SW = 700 Hz
SW = 800 Hz
I/I0
I28
L29
N30
S32
E33
G34
D35
W36
0.0
0.2
0.4
0.6
136
132
128
124
120
116
112
108
104
15N (ppm)

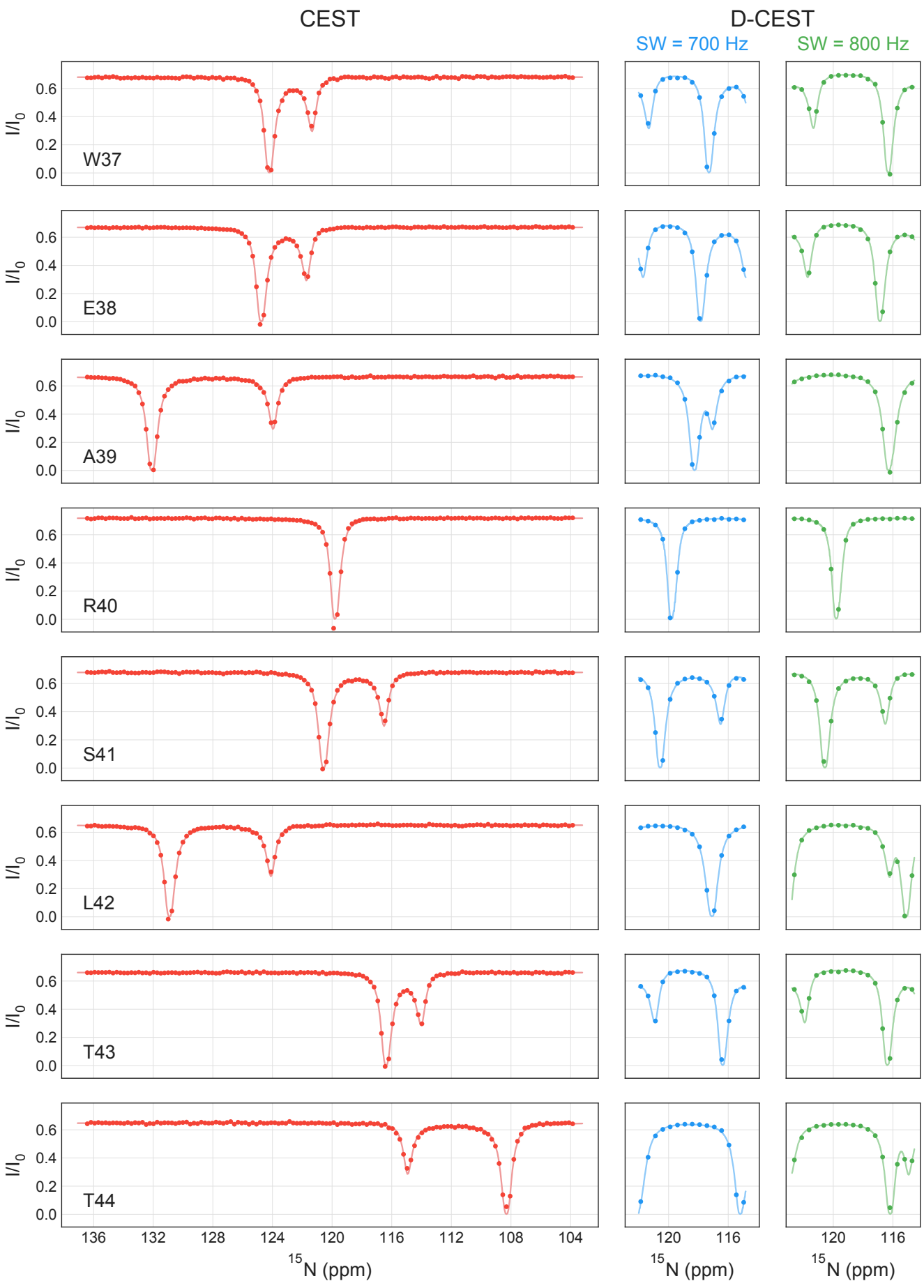
CEST
D-CEST
SW = 700 Hz
SW = 800 Hz
I/I0
W37
E38
A39
R40
S41
L42
T43
T44
0.0
0.2
0.4
0.6
136
132
128
124
120
116
112
108
104
120
116
120
116
15N (ppm)
15N (ppm)
15N (ppm)

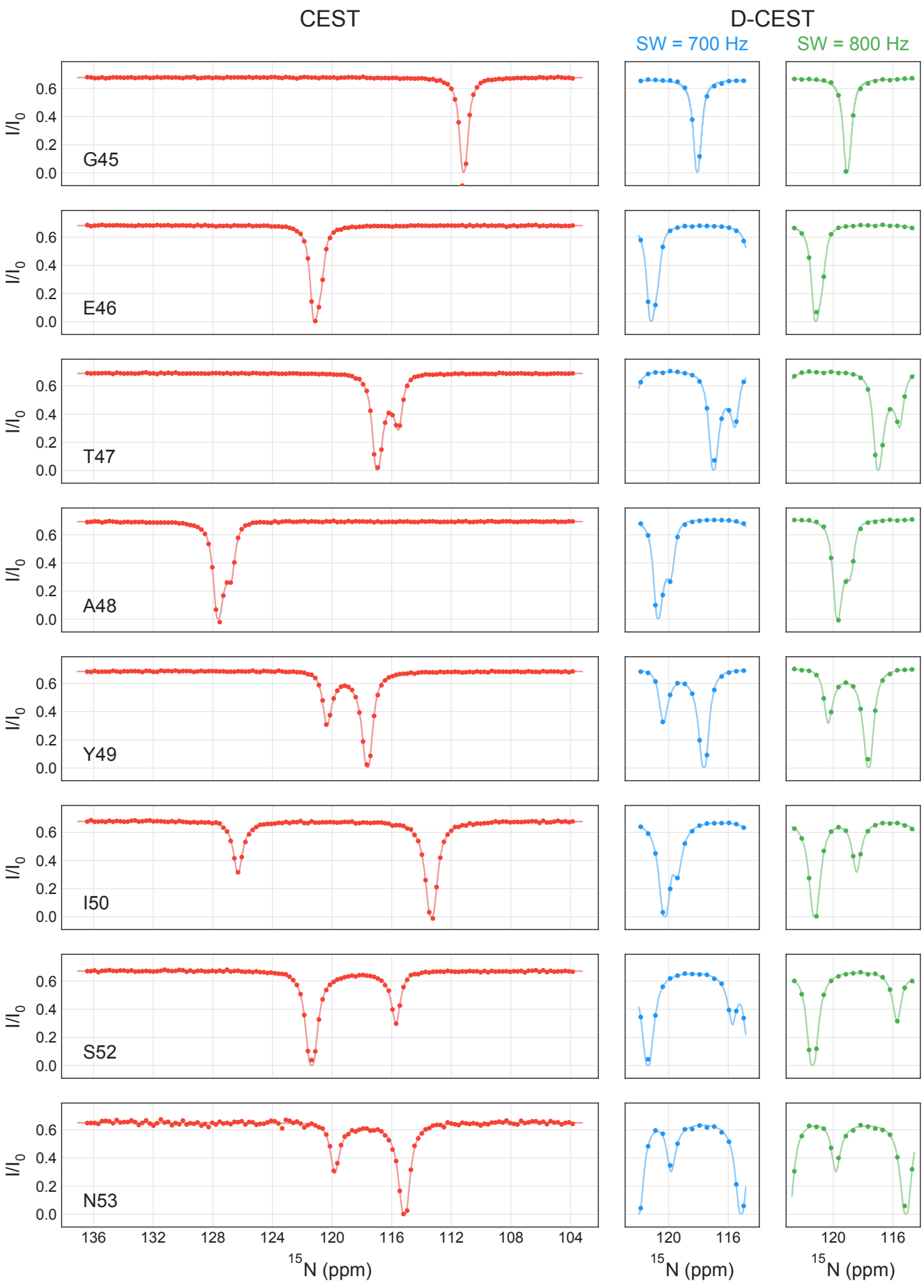
CEST
D-CEST
SW = 700 Hz
SW = 800 Hz
I/I0
0.0
0.2
0.4
0.6
G45
E46
T47
A48
Y49
I50
S52
N53
136
132
128
124
120
116
112
108
104
120
116
120
116
15N (ppm)
15N (ppm)
15N (ppm)

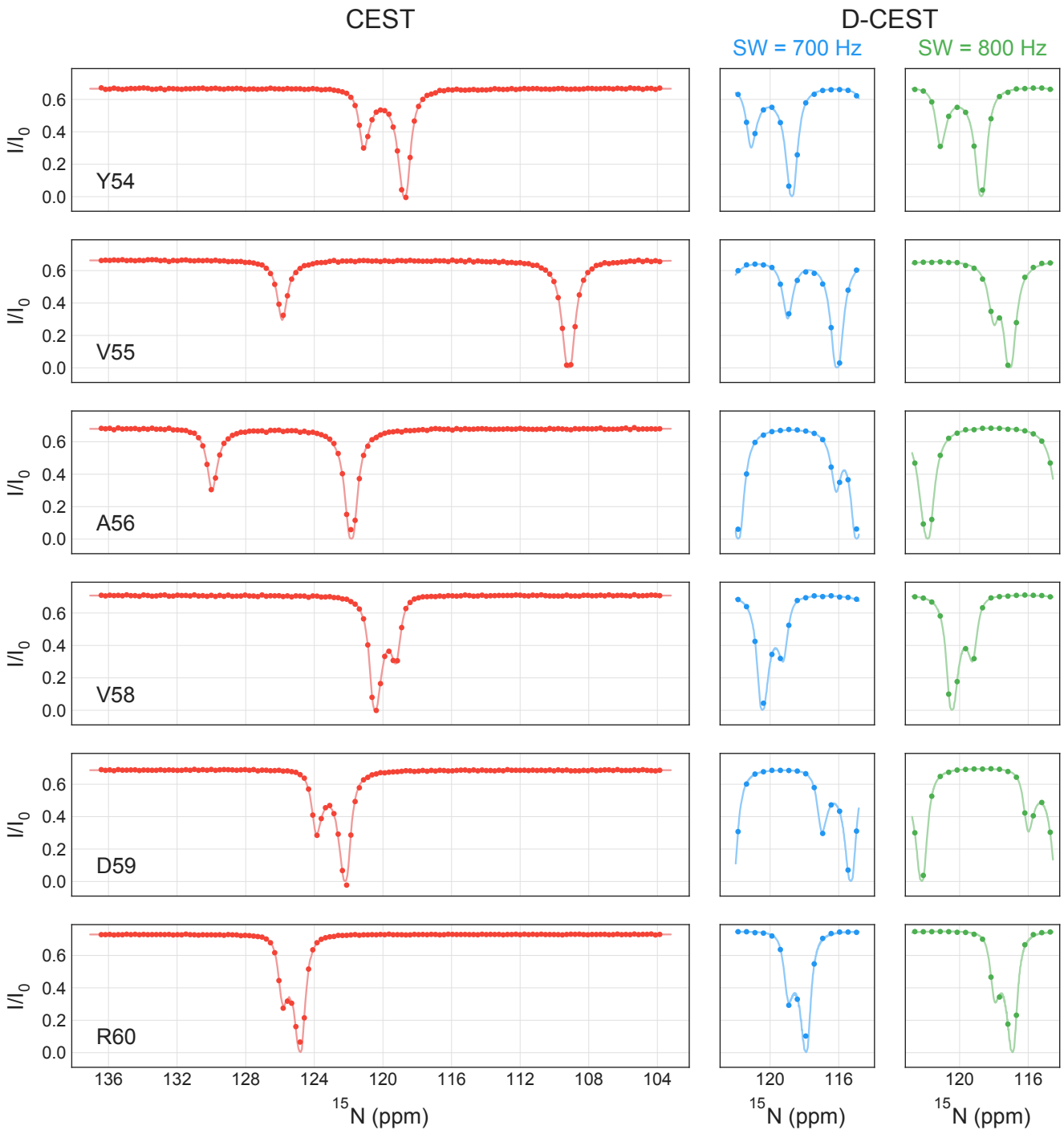
CEST
D-CEST
SW = 700 Hz
SW = 800 Hz
I/I0
Y54
V55
A56
V58
D59
R60
0.0
0.2
0.4
0.6
136
132
128
124
120
116
112
108
104
120
116
120
116
15N (ppm)
15N (ppm)
15N (ppm)

Figure S6 ***(previous pages).*** ^{15}N-CEST profiles of the G48A Fyn SH3 domain recorded at 25 °C, 23.5 T, using the standard ^{15}N-CEST pulse sequence (red) and the ^{15}N D-CEST pulse sequence with sw_{CEST} set to 700 Hz (blue) and 800 Hz (green). All experiments were recorded with the same carrier position (~118.7 ppm) with B_1 offset ranges in the CEST (sw = 3300 Hz), D-CEST (sw = 700 Hz) and D-CEST (sw = 800 Hz) datasets of $[-1500, 1800]$ Hz, $[-375, 325]$ Hz and $[-400, 400]$ Hz, respectively. Experimental data points are shown with circles along with best fits of data (solid lines). D-CEST datasets were jointly analyzed as described in the "*Data analysis*" section. All experiments were recorded using an effective B_1 field of 20 Hz.

References

[1] H. M. McConnell, *J. Chem. Phys.* **1958**, *28*, 430–431.

[2] M. H. Levitt, *J. Magn. Reson.* **1985**, *50*, 95–110.

[3] P. Vallurupalli, G. Bouvignies, L. E. Kay, *J. Am. Chem. Soc.* **2012**, *134*, 8148–8161.

[4] P. Vallurupalli, A. Sekhar, T. Yuwen, L. E. Kay, *J. Biomol. NMR* **2017**, *67*, 243–271.

[5] G. Bouvignies, P. Vallurupalli, L. E. Kay, *J. Mol. Biol.* **2014**, *426*, 763–774.

[6] M. Guenneugues, P. Berthault, H. Desvaux, *J. Magn. Reson.* **1999**, *136*, 118–126.

[7] F. Delaglio, S. Grzesiek, G. W. Vuister, G. Zhu, J. Pfeifer, A. Bax, *J. Biomol. NMR* **1995**, *6*, 277–293.

[8] T. D. Goddard, D. G. Kneller, *SPARKY 3, University of California, San Francisco*, **2008**.

[9] W. Lee, M. Tonelli, J. L. Markley, *Bioinformatics* **2015**, *31*, 1325–1327.

[10] M. Helgstrand, T. Härd, P. Allard, *J. Biomol. NMR* **2000**, *18*, 49–63.

[11] T. Yuwen, G. Bouvignies, L. E. Kay, *J. Magn. Reson.* **2018**, *292*, 1–7.

```
/* N15DCEST_gd_enh_lek_800_cp

   Pulse scheme to record 15N D-CEST scheme
     Set time_T1 to typically 300-1000 ms and vary 15N saturation frequency

   Use gen_fq3list.py to generate the 15N frequency list (fq3list)
   Use gen_vclist.py to generate the vclist for B1 calibration

   To calibrate 15N B1eff field: set -Dcal_NB1
   1. Use -DF2P and set FnMODE(F2) to 'States' for B1 calibration experiment
      that keeps only one quadrature component rather than a pair of doublets.
      Such scheme is useful for calibrating small B1eff (< 10 Hz), TD(F2)
      should be set as twice the number of points in 'vclist'
   2. Use -Dcp_flg to carry out selective het-cp (two-way) and excite only
      one single peak, cnst1 and cnst3 should be set to the position of 1H
      and 15N for the peak of interest respectively. The het-cp power cnst6
      should be set as 35~40 Hz to achieve good selectivity

   For -Dcp_flg (without -Dcal_NB1), het-CP total transfer time: 28.778*pw_dip*l3,
     typically set ~4 kHz power for het-cp (pw_dip ~60 us), and l3 set to ~6
     in order to achieve tau_cp ~10.8 ms (= 1/JNH)

   Use -DHdec_adj to automatically adjust 1H decoupling power, such that
     decoupling sidebands fold onto the position of major dip. cnst5 should be
     set properly reflecting the total degrees of rotation made by one unit

   Modified by TY on Oct 22, 2017 based on N15CEST_gd_enh_800_lek_v2_cp

   Modified by TY on Oct 27, 2017 to add the option of performing CaWurst
   decoupling on 13C during CEST period

*/

;prosol relations=<triple>
;aqseq 321

#include <Avance.incl>
#include <Grad.incl>
#include <Delay.incl>

/***********************/
/*   Define phases     */
/***********************/
#define zero ph=0.0
#define one ph=90.0
#define two ph=180.0
#define three ph=270.0

/***********************/
/*   Define delays     */
/***********************/
define delay hscuba      /* length of 1/2 scuba delay */
  "hscuba=30m"

#ifndef cal_NB1
  define delay time_T1
    "time_T1=d2"
  define delay time_T1_max
    "time_T1_max=d3"

  define delay time_T1_adj
  define delay time_T1_max_adj
#endif

define delay taua        /* 1 / 4J(XH)                */
  "taua=d4"              /* use JNH=105 to decreas the tauxh duration */
define delay taub        /* 1 / 4J(XH)                */
  "taub=d5"              /* use 1/4J(XH=95Hz)         */
define delay BigT1
  "BigT1=d14"

"d11=30m"
"in0=inf1/2"             /* t1/2 increment */
```

```
"TAU2=0.2u"

#ifdef ip_flg
  define delay t1_max

  define loopcounter ni
    "ni=td1/2"
#endif

/*****************************************************************/
/* f1180: Start t1 at half dwell to get -90/180 phase correction */
/*        in F1 (15N) dim - set zgoptns -Df1180                  */
/*****************************************************************/
#if defined(f1180) && !defined(cal_NB1)
  "d0=(in0/2)"
#else
  "d0=0.2u"
#endif

/************************/
/*   Define pulses      */
/************************/
define pulse dly_pg1     /* Messerle purge pulse*/
  "dly_pg1=5m"
define pulse dly_pg2     /* Messerle purge pulse*/
  "dly_pg2=dly_pg1/1.62"
define pulse pwh
  "pwh=p1"               /* 1H hard pulse at power level pl1 (tpwr) */
define pulse pwn
  "pwn=p3"               /* PW90 for N pulse at power level pl3 (dhpwr2)  */

#ifdef cp_flg
  define pulse pw_dip
#ifdef cal_NB1
    "pw_dip=taub*4.0"    /* set to 10.8 ms for complete H to N transfer */
#else
    "pw_dip=p16"         /* set to ~ 62.5 us so that tau_cp = 10.8 ms */
#endif
#else
#ifdef N_sel
  define pulse pwn_sl
    "pwn_sl=p32"
#endif
#endif

#ifdef c_flg
  define pulse pwc_ad
    "pwc_ad=p22"         /* pwc_ad at sp22 (d_ad)   */
#endif

define pulse pwn_dante
  "pwn_dante=p34"

/**********************/
/*    Define lists    */
/**********************/
#ifdef cal_NB1
  define list<loopcounter> ncyc_cal=<$VCLIST>
#else
  define list<frequency> N_offset=<$FQ3LIST>
#endif

/*****************************************************/
/* Assign cnsts to check validity of parameter range */
/*****************************************************/
#ifdef fsat
  "cnst10=plw10"         /* tsatpwr - set max at 0.00005W */
#endif

#ifdef cp_flg
#ifdef cal_NB1
  "plw16=plw12*pow((p12*4.0*cnst6)/1s,2)"
  "plw35=plw3*pow((pwn*4.0*cnst6)/1s,2)"
```

```
#else
  "plw16=plw12*pow(p12/pw_dip,2)"
  "plw35=plw3*pow(pwn/pw_dip,2)"

  define delay tau_cp
    "tau_cp=(2590.0/90.0)*pw_dip*l3"
#endif

  "cnst16=plw16"
  "cnst35=plw35"
#else
#ifdef N_sel
  "cnst32=spw32"
#endif
#endif

#ifdef c_flg
  "cnst22=spw22"          /* d_ad - set max at 80W" */
#endif

#ifdef cawurst_flg
  "spw23=plw23"
  "cnst23=plw23"          /* dpwrcadec - set max at 6.0W */
#endif

"cnst31=plw31"            /* dpwr2 - set max at 6W */
"cnst34=plw34"            /* 15N power level for DANTE pulses */

/***********************************/
/* Calculate parameters for D-CEST */
/***********************************/
define pulse p_dante
  "p_dante = (4.0*pwn_dante*cnst9)/cnst8"

define delay d_dante
  "d_dante = 1s/cnst8 - p_dante"

#ifndef cal_NB1
  "l4 = (trunc((time_T1/1s)*cnst8+0.1))"
  "time_T1_adj = 1s*(l4/cnst8)"
  "time_T1_max_adj = larger(time_T1_adj, time_T1_max)"
#endif

/************************************************/
/* Make adjustment for 1H decoupling power level */
/************************************************/
#ifdef Hdec_adj
  "l5 = trunc((1s*90.0)/(2.0*p12*cnst5*cnst8) + 0.5)"
  "p15 = (1s*90.0)/(2.0*l5*cnst5*cnst8)"
  "plw15 = pow(p12/p15,2)*plw12"
#else
  "p15 = p12"
  "plw15 = plw12"
#endif

"cnst12=plw15"            /* tpwrml - set max at 5W" */

/************************/
/* Initialize variables */
/************************/
"l2=0"
"plw2=0"
"spoal22=0.5"
"spoff22=0"

;"acqt0 = 0"
;baseopt_echo

/******************************/
/* BEGIN ACTUAL PULSE SEQUENCE */
/******************************/
1 ze
/***************************************/
```

```
/*   Check Validity of Parameter Range   */
/***************************************/
#ifdef fsat
  if "cnst10 > 0.00005" {
    2u
    print "error: tsatpwr pl10 is too high; < 0.00005W !!!"
    goto HaltAcqu
  }
#endif

  if "cnst12 > 5" {
    2u
    print "error: tpwrml pl12 is too high; < 5W !!!"
    goto HaltAcqu
  }

#ifdef cp_flg
  if "cnst16 > 4" {
    2u
    print "error: pl16 is too high; < 4W !!!"
    goto HaltAcqu
  }

  if "cnst35 > 60" {
    2u
    print "error: pl35 is too high; < 60W !!!"
    goto HaltAcqu
  }

#ifndef cal_NB1
  if "tau_cp > 14m" {
    2u
    print "error: dipsi-2 het-cp duration is too long; < 14ms !!!"
    goto HaltAcqu
  }

  if "tau_cp < 6m" {
    2u
    print "error: dipsi-2 het-cp duration is too short; > 6ms !!!"
    goto HaltAcqu
  }
#endif
#else
#ifdef N_sel
  if "cnst32 > 60" {
    2u
    print "error: dpwr2_sl spw32 is too high; < 60W !!!"
    goto HaltAcqu
  }
#endif
#endif

#ifdef c_flg
  if "cnst22 > 80" {
    2u
    print "error: d_ad pl22 is too high; < 80W !!!"
    goto HaltAcqu
  }
#endif

#ifdef cawurst_flg
  if "cnst23 > 8" {
    2u
    print "error: dpwrcadec pl23 is too high; < 8W !!!"
    goto HaltAcqu
  }
#endif

  if "cnst9/cnst8 > 0.25" {
    2u
    print "error: N15_B1/N15_SW ratio is too large; < 0.25 !!!"
    goto HaltAcqu
  }
```

```
  if "cnst31 > 9" {
    2u
    print "error: dpwr2 pl31 is too high; < 9W !!!"
    goto HaltAcqu
  }

#ifndef cal_NB1
  if "time_T1 > 1000m" {
    2u
    print "error: time_T1 is too long; < 1000ms !!!"
    goto HaltAcqu
  }

  if "time_T1_max > 1100m" {
    2u
    print "error: time_T1_max is too long; < 1100ms !!!"
    goto HaltAcqu
  }
#endif

  if "aq > 100m" {
    2u
    print "error: aq is too long; < 100ms !!!"
    goto HaltAcqu
  }

  if "d1 < 1.5s" {
    2u
    print "error: d1 is too short; > 1.5s !!!"
    goto HaltAcqu
  }

2 d11 do:f3              /* loop back to here - NS times (per fid) */
  2u rpp11 rpp12
/*****************************************/
/* Continue with checks that are run time */
/*****************************************/
#ifdef cal_NB1
  if "ncyc_cal/cnst8 > 2.0" {
    2u
    print "error: evolution time during B1 cal is too long !!!"
    goto HaltAcqu
  }
#endif

/***********************************************/
/* H heat compensation period - always do this  */
/***********************************************/
  10u fq=cnst1:f1        /* 1H SFO1+cnst1(Hz) @ tofNH */
  4u pl15:f1             /* power for 1H decoupling */
  (2u cpds1 ph26):f1     /* 1H dec ON */

#ifndef cal_NB1
  if "abs(N_offset) > 10000Hz" {
    time_T1_max_adj
  }
  else {
    if "time_T1_adj < time_T1_max_adj" {
      "DELTA = time_T1_max_adj - time_T1_adj"
      DELTA
    }
  }
#endif

  2u do:f1               /* 1H dec off */

/***********************************************/
/* Destroy residual 1H magnetization prior to d1 */
/***********************************************/
  10u fq=0:f1            /* 1H SFO1 @ tof(water) */
  4u pl1:f1              /* power pl1 for 1H pulses */
  20u UNBLKGRAD
```

```
  (pwh ph26):f1

  2u
  p50:gp0*0.5
  d16

  (pwh ph27):f1

  2u
  p50:gp0
  d16

  4u BLKGRAD

#ifdef mess_flg
  4u pl11:f1
  (dly_pg1 ph26):f1
  2u
  (dly_pg2 ph27):f1
#endif

#ifdef fsat
  4u pl10:f1
  d1 cw:f1 ph26
  2u do:f1
  4u pl1:f1
#ifdef fscuba
  hscuba
  (pwh ph26):f1
  (pwh*2 ph27):f1
  (pwh ph26):f1
  hscuba
#endif /*fscuba*/
#else  /*fsat*/
  4u pl1:f1
  d1
#endif /*fsat*/
  20u UNBLKGRAD

/*************************************************/
/* Eliminate all magnetization originating on 15N */
/*************************************************/
  4u pl3:f3
  (pwn ph26):f3

  2u
  p50:gp0
  d16

/*************************/
/* This is the real start */
/*************************/
#ifdef cp_flg
  10u fq=cnst1:f1

#ifdef cal_NB1
  10u fq=cnst3:f3
#endif

  (pwh ph26):f1
  2u pl16:f1 pl35:f3

#ifdef cal_NB1
  (center (pw_dip ph27):f1 (pw_dip ph27):f3)
#else
3 (center (pw_dip*3.556 ph11):f1 (pw_dip*3.556 ph11):f3)
  (center (pw_dip*4.556 ph12):f1 (pw_dip*4.556 ph12):f3)
  (center (pw_dip*3.222 ph11):f1 (pw_dip*3.222 ph11):f3)
  (center (pw_dip*3.167 ph12):f1 (pw_dip*3.167 ph12):f3)
  (center (pw_dip*0.333 ph11):f1 (pw_dip*0.333 ph11):f3)
  (center (pw_dip*2.722 ph12):f1 (pw_dip*2.722 ph12):f3)
  (center (pw_dip*4.167 ph11):f1 (pw_dip*4.167 ph11):f3)
```

```
  (center (pw_dip*2.944 ph12):f1 (pw_dip*2.944 ph12 ipp12):f3)
  (center (pw_dip*4.111 ph11):f1 (pw_dip*4.111 ph11 ipp11):f3)
  lo to 3 times l3
#endif

  2u pl3:f3
  (pwn ph1):f3

  10u fq=0:f1
#else /*cp_flg*/
  (pwh ph26):f1

  2u
  p51:gp1
  d16

#ifdef N_sel
  "DELTA = taua - 2u - p51 - d16 - pwn_sl*0.5"
  DELTA

  (center (pwh*2 ph26):f1 (pwn_sl:sp32 ph26):f3)
#else
  "DELTA = taua - 2u - p51 - d16"
  DELTA

  (center (pwh*2 ph26):f1 (pwn*2 ph26):f3)
#endif

  DELTA pl3:f3

  2u
  p51:gp1
  d16

  (pwh ph27):f1

  2u
  p52:gp2
  d16

  (pwn ph1):f3

  2u
  p53:gp3
  d16

  "DELTA = taub - 2u - p53 - d16"
  DELTA

  (center (pwh*2 ph26):f1 (pwn*2 ph26):f3)

  DELTA

  2u
  p53:gp3
  d16

  (pwn ph27):f3
  2u
  (pwh ph26):f1
#endif /*cp_flg*/

  2u
  p54:gp4
  d16

/*******************************************/
/* Start time_T1 relaxation/exchange period */
/*******************************************/
  10u fq=cnst1:f1
  4u pl15:f1 pl34:f3

#ifdef cawurst_flg
```

```
  4u pl23:f2
  (2u cpds2 ph26):f2
#endif

  (2u cpds1 ph26):f1

#ifdef cal_NB1
  10u fq=cnst3:f3

#ifdef F2P
  (pwn_dante ph26):f3
#endif

  if "ncyc_cal > 0" {
4   (p_dante ph26):f3
    d_dante
    lo to 4 times ncyc_cal
  }

#ifdef F2P
  if "l2 % 2 == 0" {
    (pwn_dante ph28):f3
  }
#endif

#else /*cal_NB1*/
  10u fq=N_offset:f3

  if "abs(N_offset) <= 10000Hz" {
    if "l4 > 0" {
4     (p_dante ph26):f3
      d_dante
      lo to 4 times l4
    }
  }
#endif /*cal_NB1*/

  2u do:f1

#ifdef cawurst_flg
  2u do:f2
#endif

  10u fq=0:f1 fq=0:f3
  4u pl11:f1 pl3:f3

  (dly_pg1 ph26):f1
  2u
  (dly_pg2 ph27):f1

  2u
  p55:gp5
  d16

/*********************************/
/* 15N Frequency labeling period */
/*********************************/
#ifdef ip_flg
  "t1_max = (ni-1)*in0*2.0 + in0 + 2u"

  10u fq=cnst1:f1
  4u pl12:f1
  (2u cpds5 ph26):f1

  "DELTA = larger(t1_max-d0*2.0, TAU2)"
  DELTA                 /* compensate to ensure same amount of 1H heating for all d
0 */

  (pwn ph2):f3

#ifdef c_flg
  if "d0 - pwc_ad*0.5 > 2u" {
    "DELTA = d0 - pwc_ad*0.5"
```

```
    DELTA
    (pwc_ad:sp22 ph26):f2
    DELTA
  }
  else {
    d0
    d0
  }
#else
  d0
  d0
#endif /*c_flg*/

  2u do:f1
  10u fq=0:f1
  4u pl1:f1

  2u
  p56:gp6*-1.0
  d16

  "DELTA = taub - 2u - 10u - 4u - 2u - p56 - d16"
  DELTA

  (center (pwh*2 ph26):f1 (pwn*2 ph3):f3)

  "DELTA = taub - 2u - p56 - d16"
  DELTA

  2u
  p56:gp6*1.0
  d16
#else /*ip_flg*/
  (pwn ph2):f3

  2u
  p56:gp6*-1.0
  d16

  "DELTA = taub + pwh*2.0 - 2u - p56 - d16"
  DELTA pl1:f1

  (pwn*2 ph3):f3

  d0

  (pwh*2 ph26):f1

  2u
  p56:gp6
  d16

#ifdef c_flg
  "DELTA = taub - 2u - p56 - d16 - pwc_ad"
  DELTA
  (pwc_ad:sp22 ph26):f2
#else
  "DELTA = taub - 2u - p56 - d16"
  DELTA
#endif

  d0
#endif /*ip_flg*/

#if defined(cp_flg) && defined(cal_NB1)
  10u fq=cnst1:f1 fq=cnst3:f3
  (ralign (pwh ph26):f1 (pwn ph26):f3)

  2u pl16:f1 pl35:f3
  (center (pw_dip ph27):f1 (pw_dip ph27):f3)

  2u pl1:f1
  (pwh ph26):f1
```

```
  10u fq=0:f1 fq=0:f3

  "DELTA = BigT1 - 10u"
  DELTA
#else
  (center (pwh ph26):f1 (pwn ph4):f3)

  2u
  p57:gp7
  d16

  "DELTA = taua - 2u - p57 - d16"
  DELTA

  (center (pwh*2 ph26):f1 (pwn*2 ph26):f3)

  DELTA

  2u
  p57:gp7
  d16

  (center (pwh ph27):f1 (pwn ph29):f3)

  2u
  p58:gp8
  d16

  "DELTA = taua - 2u - p58 - d16"
  DELTA

  (center (pwh*2 ph26):f1 (pwn*2 ph26):f3)

  "DELTA = taua - 2u - p58 - d16 + (pwn - pwh)*0.5"
  DELTA

  2u
  p58:gp8
  d16

  (pwh ph28):f1

  BigT1
#endif

  (pwh*2 ph26):f1

  2u
  p59:gp9*-1.0*EA
  d16

  "DELTA = BigT1 - 2u - p59 - d16 - 4u - 4u - de + pwh*2.0/PI"
  DELTA

  4u BLKGRAD
  4u pl31:f3

/****************/
/* Acquire data */
/****************/
  go=2 ph31 cpds3:f3
  d11 do:f3 mc #0 to 2

#ifdef cal_NB1
#ifdef F2P
  F2PH(calclc(l2,1), calclist(ncyc_cal,1))
#else /*cp_flg*/
  F2QF(calclist(ncyc_cal,1))
#endif /*cp_flg*/
#else /*cal_NB1*/
  F2QF(calclist(N_offset,1))
#endif /*cal_NB1*/
```

```
  F1EA(calgrad(EA) & calph(ph4, +180), caldel(d0, +in0) & calph(ph2, +180) & calph(p
h31, +180))

HaltAcqu, 1m
exit

ph1=0 2
ph2=1
ph3=0 0 1 1 2 2 3 3
ph4=0
ph11=1 3 3 1
ph12=3 1 1 3
ph26=0
ph27=1
ph28=2
ph29=3
ph31=0 2 2 0

;d1: relaxation delay
;d2: time_T1
;d3: time_T1_max
;d4: taua delay ~ 2.38 ms (< 1/4JNH)
;d5: taub delay = 2.68 ms (= 1/4JNH)
;d11: delay for disk i/o, 30ms
;d14: set to BigT1 500 us
;d16: gradient recovery delay, 200us
;tau_cp: dipsi2 het-cp duration (~1/JNH = 10.8 ms)
;pl1: tpwr - power level for pwh
;pl3: dhpwr2 - power level for 15N pulse pwn
;pl10: tsatpwr - power level for water presat
;pl11: tpwrmess - power level for Messerle purge
;pl12: tpwrml - power level for 1H decoupling during time_T1
;plw15: tpwrml - adjusted power level for 1H decoupling during time_T1
;pl23: dpwrsed - power level for Ca/CO (wurst-2) decoupling
;pl31: dpwr2 - power level for 15N cpd3
;pl34: power level for 15N DANTE pulses
;sp22: power level for pwc_ad
;sp32: power level for pwn_sl
;spnam22: shape for pwc_ad
;spnam23: File name for Ca/CO decoupling during 15N CEST period
;spnam32: shape for pwn_sl
;p1: pwh - 1H 90 degree pulse
;p3: pwn - 15N 90 degree pulse
;p12: pwmlev - 90 degree pulse for decoupling sequence
;p15: pwmlev - adjusted 90 degree pulse for decoupling sequence
;p16: pw_dip - 90 degree pulse for dipsi-2 het-cp
;p22: pwc_ad - 13C 180 pulse (adiabatic)
;p23: pwcadec - Ca/CO wurst-2 dec total length of supercycled pattern
;p32: pwn_sl for selective pulse on amide N15
;p34: pwn_dante - 90 degree pulse at pl34
;p50: gradient pulse 50                                  [1000 usec]
;p51: gradient pulse 51                                  [500 usec]
;p52: gradient pulse 52                                  [1000 usec]
;p53: gradient pulse 53                                  [500 usec]
;p54: gradient pulse 54                                  [500 usec]
;p55: gradient pulse 55                                  [1000 usec]
;p56: gradient pulse 56                                  [625 usec]
;p57: gradient pulse 57                                  [500 usec]
;p58: gradient pulse 58                                  [500 usec]
;p59: gradient pulse 59                                  [256 usec]
;cpdprg1: 1H decoupling program during 15N CEST [p90x240y90x.p15]
;cpdprg2: 13C decoupling program during 15N CEST [p5m4sp180.p23]
;cpdprg3: 15N decoupling program during t2 [waltz16]
;pcpd3: f3 channel - 90 degree pulse for decoupling sequence (1/dmf2)
;cpdprg5: 1H decoupling program during t1 [waltz16.p12]
;cnst1: diff (Hz) between 1H decoupling position and water
;cnst3: diff (Hz) between 15N peak and carrier for B1 calibration
;cnst5: amount of rotation (degree) made by each element of cpdprg1
;cnst6: weak B1 field (Hz) for het-cp selective excitation
;cnst8: Frequency period (Hz) between adjacent excitation bands
;cnst9: Average N15 B1 (Hz) during D-CEST
;fq3list: frequency list (Hz) for 15N offsets in D-CEST
;vclist: variable counter list for 15N B1 calibration in D-CEST
```

```
;l3: loop counter for dipsi-2 cycles in het-cp
;inf1: 1/SW(X) = 2*DW(X)
;in0: 1/(2*SW(x))=DW(X)
;nd0: 2
;ns: 2*n
;FnMODE: Echo-Antiecho in F1
;FnMODE: QF in F2

;use gradient ratio:    gp 6 : gp 9
;                         80 : 39.6

;for z-only gradients:
;gpz0: 20%
;gpz1: 12%
;gpz2: 90%
;gpz3: 24%
;gpz4: 70%
;gpz5: -75%
;gpz6: 80%
;gpz7: 60%
;gpz8: 15%
;gpz9: 39.6%

;use gradient files:
;gpnam0: SMSQ10.32
;gpnam1: SMSQ10.32
;gpnam2: SMSQ10.32
;gpnam3: SMSQ10.32
;gpnam4: SMSQ10.32
;gpnam5: SMSQ10.32
;gpnam6: SMSQ10.32
;gpnam7: SMSQ10.32
;gpnam8: SMSQ10.32
;gpnam9: SMSQ10.32

;zgoptns: Df1180, Dfsat, Dfscuba, Dmess_flg, Dc_flg, Dcal_NB1, DN_sel, Dcawurst_flg,
 DHdec_adj, Dip_flg, Dcp_flg, DF2P
```